Journal of Materials Chemistry

Cite this: J. Mater. Chem., 2011, 21, 15417

www.rsc.org/materials

PAPER

The structure of two new non-centrosymmetric phases of oxygen deficient bismuth manganite

A. S. Eggeman,*[a] A. Sundaresan,[b] C. N. R. Rao[b] and P. A. Midgley*[a]

Received 20th June 2011, Accepted 4th August 2011
DOI: 10.1039/c1jm12840j

The structure of two new phases in the bismuth manganite system are reported. The phases were determined by electron diffraction studies of two oxygen-deficient bulk samples. The first phase, a minority component of bulk $BiMnO_{2.94}$ forms a $n = 2$ Ruddlesden-Popper phase with space group $Cmc2_1$. The second phase, from bulk $BiMnO_{2.99}$, is an orthorhombic structure with space group $Pmn2_1$ and a unit cell approximately equal to $4 \times \sqrt{2} \times 2\sqrt{2}$ times the parent perovskite cell. Importantly both phases are non-centrosymmetric and offer further potential for multiferroic studies.

1 Introduction

Bismuth manganite, $BiMnO_3$, a perovskite-based oxide has been studied widely over recent years because of the potential for multiferroic behaviour.[1–4] A permanent magnetic dipole arises in the perovskite structure from the ferromagnetic interaction within the manganese oxide sub-lattice, whilst the lone pair of 6*s* electrons associated with the Bi ion can lead to the Bi being displaced from the equilibrium centre of the basic perovskite unit, breaking the centre of symmetry and hence allowing the possibility of a permanent electric dipole. Evidence for such multiferroic behaviour, seen clearly in, for example, $BiFeO_3$[5] has also been established in $BiMnO_{3-x}$.[6]

The accepted structure for stoichiometric bismuth manganite ($BiMnO_3$) at room temperature and pressure is a monoclinic cell with lattice parameters $a = 9.532$ Å, $b = 5.606$ Å, $c = 9.854$ Å and $\beta = 110.67°$.[1,2] However studies on non-stoichiometric manganite samples[6] have shown that deviations from this structure can occur for only very small changes in composition. In most of the literature, structural analysis is based on X-ray or neutron data and while these techniques allow structure solution and refinement to be performed with great accuracy for bulk materials, they do lack the high spatial resolution and sensitivity to weak symmetry breaking that can be achieved using electron diffraction. There is always the possibility that $BiMnO_3$ samples (especially those that are non-stoichiometric) are heterogeneous and as such different phases may contribute to one or both of the ferroelectric and ferromagnetic signals. Electron microscopy and electron diffraction enable the structures of individual phases to be probed with near nanometre spatial resolution.

2 Experimental method

Samples of bismuth manganite were prepared at 850 °C under a pressure of 4.5 GPa by the reaction of Bi_2O_3 (previously pre-heated to 700 °C in oxygen), with an appropriate mixture of MnO and MnO_2, to enable control of the oxygen content. EDAX studies were performed to ensure the correct Bi : Mn ratio of 1 : 1 in the samples.[6] TEM samples were prepared by grinding the as-prepared powder in a pestle and mortar and adding a small amount of volatile solvent (diethyl ether). A droplet of the mixture was then placed on a holey carbon TEM film and allowed to dry.

There is evidence that bismuth manganite samples exhibit a high degree of electron beam sensitivity[7] and as such the majority of electron diffraction experiments here were undertaken at 150 kV accelerating potential to reduce the possibility of knock-on damage and loss of oxygen. Diffraction experiments were performed on a Philips CM30 TEM fitted with a Nanomegas SpinningStar precession apparatus and also on a Philips CM300 FEGTEM. Precession angles used were in the range of 10–30 mrad. Diffraction patterns were recorded on Ditabis imaging plates and Kodak film. Automated diffraction tomography[8] was performed on a Tecnai F20 with data recorded on a CCD camera. We examined two non-stoichiometric samples with bulk composition $BiMnO_{2.94}$ and $BiMnO_{2.99}$.[6]

3 Results and discussion

3.1 $BiMnO_{2.94}$ – a new Ruddlesden-Popper phase

A new phase, a minority component of the highly oxygen deficient bulk sample $BiMnO_{2.94}$, offered a challenge for structural determination. The substantial difference between the structure of this new phase and any distorted, or superstructured, perovskite made the identification and indexing of zone axis patterns at first problematic. Automated diffraction tomography[8,9] was used to acquire a series of electron diffraction patterns about a single

[a]Department of Materials Science and Metallurgy, University of Cambridge, Cambridge, UK. E-mail: ase25@cam.ac.uk; pam33@cam.ac.uk
[b]Jawarhalal Nehru Centre for Advanced Scientific Research, Bangalore, India

tilt-axis and combining the data into a 3-D reciprocal space construction enabled an application of a Niggli cell reduction routine using the Dirax software.[10] This yielded an orthorhombic cell with $a = 16.8$ Å, $b = 5.51$ Å and $c = 5.45$ Å. Using this unit cell, zone axis precession electron diffraction (PED) patterns could then be indexed consistently, examples of which are shown in Fig. 1a to 1d.

These patterns indicate the following conditions for allowed reflections: from 1a) $h00$, $h = 2n$; $0k0$, $k = 2n$; $hk0$, $h + k = 2n$; and from 1c) $00l$, $l = 2n$, $h0l$, $h,l = 2n$. In addition the [100] zone axis (shown in Fig. 2) adds the further conditions $0kl$, $k = 2n$ and hkl $h + k = 2n$. Such reflection conditions allow only 2 possible orthorhombic space groups $Cmc2_1$ and $Cmcm$. To differentiate between the two space groups it is necessary to identify the whole pattern symmetry of the [100] and/or [010] zone axis, as this will differentiate between *mm2* and *mmm* point group symmetry. Fig. 2 shows a montage with (*left*) a convergent beam electron diffraction pattern recorded parallel to the [100] zone axis, and (*middle and right*) after tilting about the *c*-axis away from the zone axis to yield an 'inverse HOLZ' pattern.[11] There is evidence (indicated with arrows in Fig. 2) both in the zone axis pattern and the 'inverse HOLZ' pattern for a small breaking of the mirror symmetry across the (001) plane, confirming a *mm2* point group and thus the non-centrosymmetric space group $Cmc2_1$. The cleavage properties of this particular material meant that the majority of crystals viewed in the electron microscope were oriented with the [100] axis close to the optic axis of the microscope and where [010] orientations were found, the recorded patterns were of insufficient quality to be used for confirmation of symmetry breaking.

The cell parameters and metal atomic coordinates (determined from direct methods[12,13] and charge-flipping[14] algorithms) showed that this phase was inconsistent with a perovskite superstructure (as seen for the conventional monoclinic bismuth manganite structure), but instead the structure fitted one based on perovskite sub-cells separated by layers with a different local stoichiometry and structure. While bismuth-containing compounds can form Aurevilius phases,[15] here the structural evidence points to a $n = 2$ Ruddlesden-Popper (R–P) phase[16] ($A_3B_2O_7$) as the correct structure with perovskite (ABO_3) sub-cells separated by rock-salt (AO) structural units. Evidence for a three-layer repeat (ABO_3–AO–ABO_3) can be seen in the relatively strong row of *3k3* reflections in the [10$\bar{1}$] zone axis pattern (Fig. 1d).

A proposed structure for the $n = 2$ Ruddlesden-Popper $Bi_3Mn_2O_7$ is shown in Fig. 3, with the atomic positions listed on the right-hand side of Table 1. Starting with ideal $n = 2$ R–P positions the metal atom positions were refined using PED data. Such diffracted intensities are known not to be kinematic and so here we used an alternative refinement scheme which considers the order (or rank) of the diffracted beam rather than the intensity. This was recently proposed as a better metric of refinement for PED data than conventional methods.[17] Once a best-fit had been found for the metal atoms alone, the oxygens were then introduced into the refinement, with initial atomic co-ordinates based on an ideal R–P phase,[18] and the whole structure refined using the same 'ranking' metric. However, the insensitivity of the data to the oxygen positions led to some error in the refinement, as shown by the final uncertainty in the oxygen atom positions.

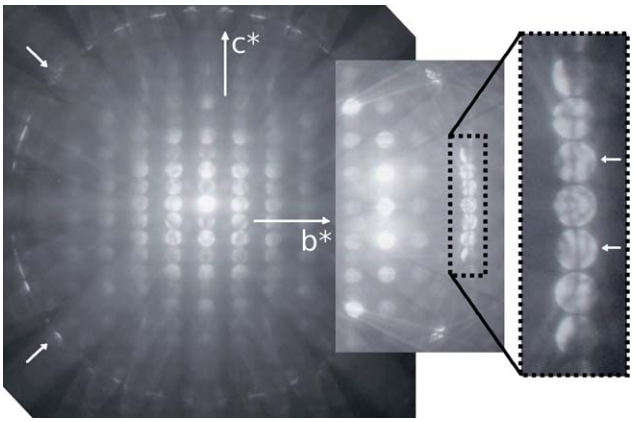

Fig. 2 Montage of convergent beam electron diffraction patterns; (*left*) recorded parallel to [100] and (*middle and right*) after tilting about the *c*-axis to an 'inverse HOLZ' condition. Arrows indicate a breaking of the mirror symmetry across the (001) plane.

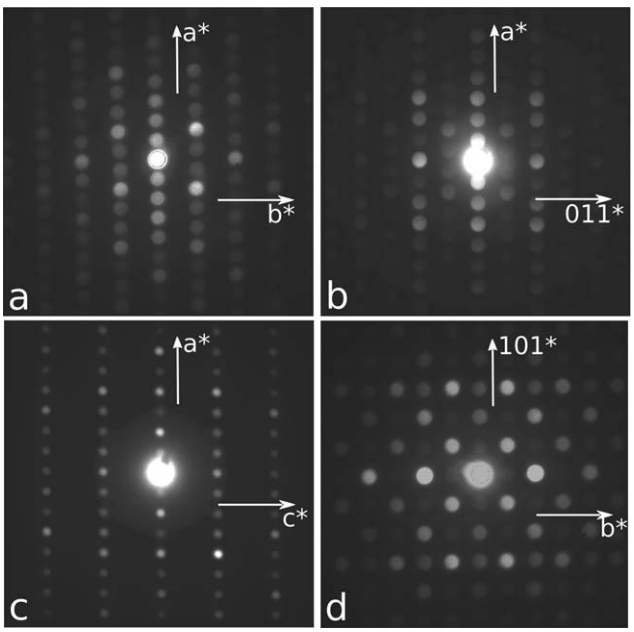

Fig. 1 Precession electron diffraction patterns from the orthorhombic phase found in the $BiMnO_{2.94}$ sample, recorded parallel to a) [001], b) [01$\bar{1}$], c) [010] and d) [10$\bar{1}$] zone axes.

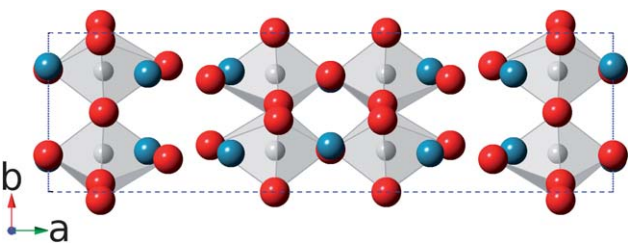

Fig. 3 The structure of the $n = 2$ Ruddlesden-Popper phase $Bi_3Mn_2O_7$ viewed along the *c*-axis. The MnO_6 octahedra are shaded, manganese are grey and the calcium are blue (colour online).

Table 1 (*left*) Atomic co-ordinates of $Ca_3Ti_2O_7$ from Elcombe *et al.*[18] and (*right*) refined atomic co-ordinates of $Bi_3Mn_2O_7$ using PED data. Errors were estimated using the approach described in Vincent *et al.*[24] Space group in both cases is $Cmc2_1$, for the bismuth manganite sample $a = 16.8$ Å, $b = 5.51$ Å and $c = 5.45$ Å

Atom	Wyckoff	x	y	z	Atom	x	y	z	Error
Ca1	4a	0.2517	0.0000	0.0290	Bi1	0.22	0.00	0.03	0.01
Ca2	8b	0.7410	0.1876	0.4747	Bi2	0.74	0.18	0.48	0.01
Ti1	8b	0.2491	0.0989	0.5000	Mn1	0.24	0.10	0.50	0.01
O1	4a	0.8124	0.0000	−0.0132	O1	0.76	0.00	−0.02	0.06
O2	8b	0.6958	0.1972	0.0132	O2	0.78	0.21	0.03	0.07
O3	8b	0.5378	0.0860	0.2883	O3	0.50	0.10	0.27	0.07
O4	8b	0.0378	0.1099	0.2117	O4	0.05	0.09	0.23	0.06

Powder X-ray diffraction of the bulk $BiMnO_{2.94}$ sample, as shown in Fig. 4, indicates that the predominant phase is the conventional monoclinic bismuth manganite, but that there are a number of additional weak peaks present that do not correspond to the monoclinic phase. Several of these peaks can be indexed based on the R–P bismuth manganite structure, as shown in the inset of Fig. 4, although there is significant overlap between many of the peaks associated with the R–P structure and the perovskite, especially at higher scattering angles. This suggests that the bulk sample is actually comprised of two different phases, a majority monoclinic ($BiMnO_3$) phase and a minority orthorhombic ($Bi_3Mn_2O_7$) phase with a $n = 2$ Ruddlesden-Popper structure. This co-existence of phases with different composition could certainly account for the apparent non-stoichiometry of the bulk sample.

3.2 $BiMnO_{2.99}$ – a new phase with an orthorhombic perovskite superstructure

The composition of the second bismuth manganite bulk sample was $BiMnO_{2.99}$, but despite the close chemical proximity to the stoichiometric ideal this phase showed a structure significantly different from the conventional monoclinic phase. Recent X-ray powder diffractometry of this sample indicated an orthorhombic phase with unit-cell parameters $2a_p \times \sqrt{2}a_p \times \sqrt{2}a_p$ (ref. 6) where a_p is the lattice parameter of the parent cubic perovskite cell. Superlattice reflections can be seen in Fig. 5a and b which show CBED patterns recorded parallel to the [010] and [100] zone axes of the orthorhombic cell. However, here the reflections indicate that the cell parameters for this structure are consistent with a cell of dimensions approximately $4a_p \times \sqrt{2}a_p \times 2\sqrt{2}a_p$, twice the cell length in two directions compared to the initial X-ray result. Careful measurement yielded unit cell parameters of $a =$ 15.6 Å, $b = 5.52$ Å and $c = 11.1$ Å. The reflections are consistent with the lattice being primitive, but Fig. 5a shows the presence of

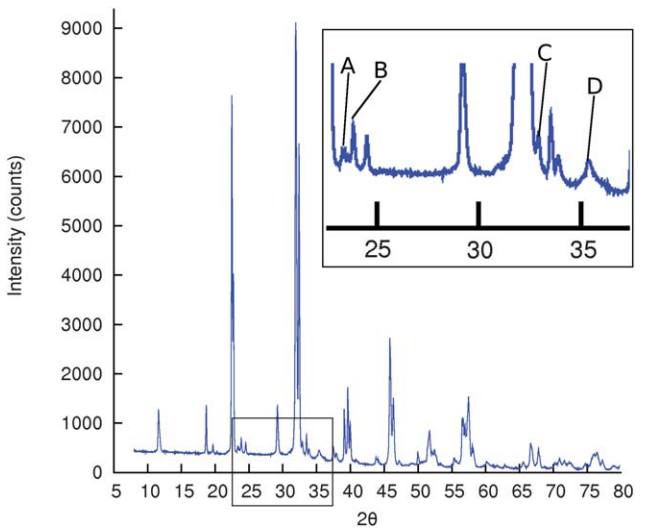

Fig. 4 Powder X-ray diffraction pattern recorded for the $BiMnO_{2.94}$ sample. The majority of the peaks correspond to those expected for the monoclinic $BiMnO_3$ phase. The inset shows several peaks indexed according to the planar spacings of the $n = 2$ Ruddlesden-Popper ($Bi_3Mn_2O_7$) phase, these are: A – 311, B – 600, C – 511 and 020 and D – 800, 021, 402 and 221.

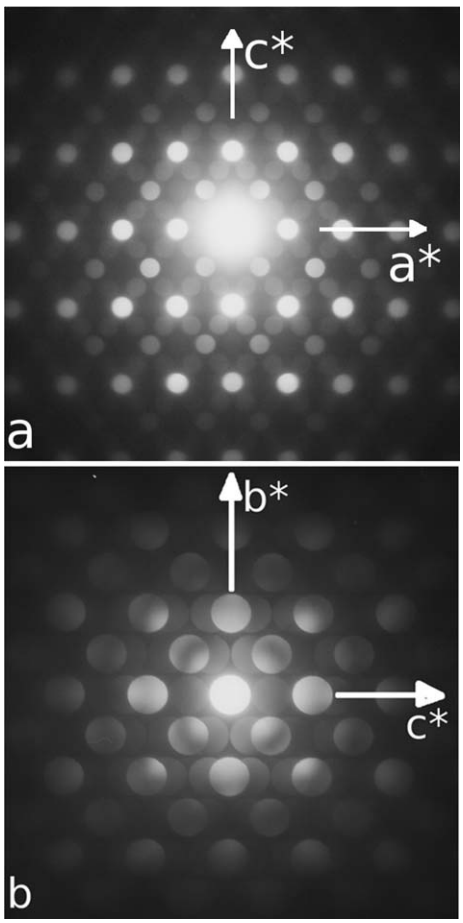

Fig. 5 Convergent beam electron diffraction patterns recorded parallel to the a) [010] and b) [100] zone axes of the $BiMnO_{2.99}$ sample.

an *n*-glide plane normal to (010), resulting in extinction conditions $h0l$, $h + l = 2n$. There are further conditions $h00$, $h = 2n$; $00l$ $l = 2n$ which lead to $Pmn2_1$ or $Pmnm$ as allowed space groups. The unit cell and space group suggests a structure similar to that of $Bi(Mn/Ni)O_3$ reported by Hughes *et al.*[19] who postulated a $Pmn2_1$ space group. A model based on this structure but using only manganese atoms is shown in Fig. 6 (with proposed atomic positions shown in Table 2).

Conclusive proof of the space group of the $BiMnO_{2.99}$ phase required careful analysis of the [100] zone axis to discover any breaking of mirror symmetry across the (001) plane. There is little evidence of such symmetry breaking in the ZOLZ layer of this zone-axis (as seen in Fig. 5b) but HOLZ reflections are more sensitive to subtle breaks in symmetry. Fig. 7 shows a wider angle view with HOLZ reflections visible in a [100] zone-axis pattern. There is some, albeit weak evidence of a lack of mirror symmetry across the (001) plane in these outer reflections (as highlighted in Fig. 7).

The lack of mirror symmetry is made much more evident after the sample is tilted about the *c*-axis away from the [100] zone axis to a minor zone axis. Here the interaction with the HOLZ reflections is much stronger (as they have a much smaller g-vector) and the appearance of HOLZ deficiency lines in the ZOLZ reflections is more evident. Fig. 8 shows a pattern recorded after tilting approximately 21° away from the [100] axis, close to the [670] zone axis. The convergence angle is such that the 002 and $00\bar{2}$ reflections dominate. These reflections are coupled by the strong 004 reflection and, given the likely four times repeat of the sub-lattice in the *c*-direction this 004 vector is likely to be very sensitive to symmetry breaking across the (001) plane. In Fig. 8 there is indeed significant symmetry breaking across the (001) plane both in the $002/00\bar{2}$ pair and also in the HOLZ reflections. The lack of mirror symmetry supports *mm2* as the point group and indicates that $Pmn2_1$ is the space group, in agreement with the phase proposed by Hughes *et al.*

3.3 Discussion

It is clear from previous studies that bulk materials with the two compositions studied here exhibit stable magnetic polarisation.[6]

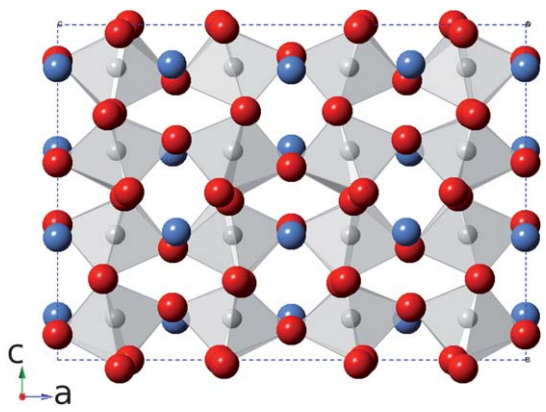

Fig. 6 Structural model of the orthorhombic $BiMnO_{2.99}$ phase (atomic positions based on Hughes *et al.*[19]) viewed along the *b*-axis. The MnO_6 octahedra are shaded, the manganese are coloured grey and the bismuth are coloured blue (colour online).

Table 2 Atomic positions for $BiMnO_{2.99}$ based on the $Bi(Mn/Ni)O_3$ structure proposed by Hughes *et al.*[19] Space group $Pmn2_1$. $a = 15.6$ Å, $b = 5.52$ Å and $c = 11.1$ Å

Atom	Wyckoff	*x*	*y*	*z*
Bi1	2a	0.000	0.0177	0.1285
Bi2	2a	0.000	0.4702	0.8692
Bi3	2a	0.000	0.5269	0.3751
Bi4	2a	0.000	0.9774	0.6348
Bi5	4b	0.7546	0.9686	0.1183
Bi6	4b	0.7469	0.4771	0.8793
Mn1	4b	0.1234	0.4937	0.6267
Mn2	4b	0.8766	0.0149	0.8774
Mn3	4b	0.6266	0.0097	0.8759
Mn4	4b	0.8741	0.5074	0.1279
O1	4b	0.1531	0.7200	0.4995
O2	4b	0.2467	0.4410	0.6660
O3	4b	0.8929	0.6890	0.2708
O4	4b	0.8460	0.2680	0.0009
O5	4b	0.8668	0.8050	0.0249
O6	4b	0.9026	0.7630	0.7592
O7	4b	0.9020	0.2700	0.7570
O8	4b	0.7546	0.0620	0.8430
O9	4b	0.6165	0.7080	0.7640
O10	4b	0.6436	0.8060	0.0121
O11	2a	0.5000	0.0700	0.9120
O12	2a	0.0000	0.5440	0.596
O13	2a	0.0000	0.4720	0.1070
O14	2a	0.0000	0.0410	0.9250

There is a strong case for orbital ordering as the mechanism for ferromagnetic behaviour[1] in the large orthorhombic structure of the $BiMnO_{2.99}$ phase in this study. The large magnetic response of the bulk $BiMnO_{2.94}$ sample suggests that the majority phase does exhibit ferromagnetism, but it is unclear at this stage whether this is true also for the minority Ruddlesden-Popper phase, $Bi_3Mn_2O_7$. There is however, evidence of stable antiferromagnetic or ferromagnetic behaviour in other manganite systems that assume the $n = 2$ Ruddlesden-Popper structure.[20,21]

Of perhaps greater importance for potential multiferroic applications is understanding the nature and origin of

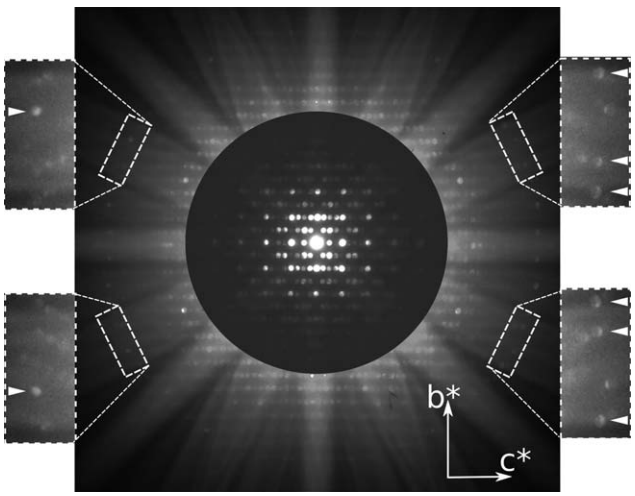

Fig. 7 Composite electron diffraction pattern recorded parallel to the $BiMnO_{2.99}$ phase [100] zone axis, showing mirror symmetry breaking in the HOLZ reflections.

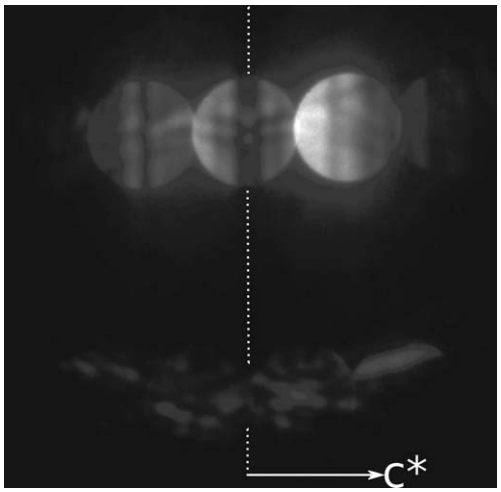

Fig. 8 CBED disks recorded after tilting away from the $BiMnO_{2.99}$ [100] zone axis, by 21° along [010]. The dotted line indicates the broken mirror symmetry across the (001) plane.

ferroelectricity in these samples. Previously, polarisation experiments showed that both bulk bismuth manganite samples studied here exhibit ferroelectric behaviour.[6] The single phase $BiMnO_{2.99}$ sample exhibits ferroelectricity, which supports the evidence in the diffraction studies in favour of the non-centrosymmetric $Pnm2_1$ space group. The correspondence between this structure and the large polar Ni-doped oxide structure reported by Hughes *et al.*[19] can be explained by considering that an oxygen vacancy can be accommodated by a reduction in the manganese oxidation state, in a way similar to the change in oxidation state brought about by the substitution of a divalent cation, such as nickel. In our case the oxygen deficiency is small (1 in 300) but seems to be sufficient to stabilise this structure.

The $BiMnO_{2.94}$ bulk sample is a more difficult case to assess because of the mixed phase nature of the sample. The very small reported electric dipole of the bulk sample could be explained by it originating in the non-centrosymmetric Ruddlesden-Popper minority phase, $Bi_3Mn_2O_7$ (space group $Cmc2_1$), with the remainder of the sample having a non-polar monoclinic space group (possibly $C2/c$) and so contributing nothing to the electric polarisation per unit mass. There is still some debate surrounding the centrosymmetry of the monoclinic phase of bismuth manganite[22] and electron diffraction studies are currently in progress to confirm any symmetry breaking. With regard to a possible ferroelectric signal in the R–P phase it is worth noting the recent article by Benedek and Fennie[23] which discusses the possibility of 'hybrid improper' ferroelectric behaviour in $Ca_3Mn_2O_7$ (the calcium analogue of the R–P bismuth manganite phase discussed here).

4 Conclusions

Two new crystal structures have been discovered within the bismuth manganite system from samples with a bulk composition of $BiMnO_{3-x}$. These have been investigated using a variety of electron diffraction techniques and from which, information about the unit-cell parameters, space group and atomic co-ordinates of the structures has been determined. The first new phase is a $n = 2$ Ruddlesden-Popper structure with space group $Cmc2_1$, while the second new phase is a perovskite superstructure with space group $Pmn2_1$. Both phases have non-centrosymmetric structures which supports the possibility of multiferroic behaviour. Further studies are underway to grow and characterise single-crystal samples of the new phases to enable bulk analysis of their magnetic and electric properties.

References

1 T. Atou, H. Chiba, K. Ohoyama, Y. Yamaguchi and Y. Syono, *J. Solid State Chem.*, 1999, **145**, 639–642.
2 A. A. Belik, S. Iikubo, T. Yokosawa, K. Kodama, N. Igawa, S. Shamoto, M. Azuma, M. Takano, K. Kimoto, Y. Matsui and E. Takayama-Muromachi, *J. Am. Chem. Soc.*, 2007, **129**, 971–977.
3 A. Moreira dos Santos, S. Parashar, A. R. Raju, Y. S. Zhou, A. K. Cheetham and C. N. R. Rao, *Solid State Commun.*, 2002, **122**, 49–52.
4 A. Moreira dos Santos, A. K. Cheetham, T. Atou, Y. Syono, Y. Yamaguchi, K. Ohoyama, H. Chiba and C. N. R. Rao, *Phys. Rev. B: Condens. Matter*, 2002, **66**, 064425.
5 J. Wang, J. B. Neaton, H. Zheng, V. Nagarajan, S. B. Ogale, B. Liu, D. Viehland, V. Vaithyanathan, D. G. Schlom, U. V. Waghmare, N. A. Spaldin, K. M. Rabe, M. Wuttig and R. Ramesh, *Science*, 2003, **299**, 1719–1722.
6 A. Sundaresan, R. V. K. Mangalam, A. Iyo, Y. Tanaka and C. N. R. Rao, *J. Mater. Chem.*, 2008, **18**, 2191–2197.
7 H. Yang, Z. H. Chi, F. Y. Li, C. Q. Jin and R. C. Yu, *Phys. Rev. B: Condens. Matter Mater. Phys.*, 2006, **73**, 024114.
8 U. Kolb, T. Gorelick, C. Kübel, M. T. Otten and D. Hubert, *Ultramicroscopy*, 2007, **107**, 507–513.
9 T. A. White, PhD thesis, University of Cambridge, 2009.
10 A. J. M. Duisenberg, *J. Appl. Crystallogr.*, 1992, **25**, 92–96.
11 C. J. Rossouw, C. J. Maunders, H. J. Whitfield and J. Etheridge, *Ultramicroscopy*, 2006, **106**, 439–448.
12 J. Gillis, *Acta Crystallogr.*, 1948, **1**, 76–80.
13 D. Harker and J. Kasper, *Acta Crystallogr.*, 1948, **1**, 70–75.
14 G. Oszlanyi and A. Suto, *Acta Crystallogr., Sect. A: Found. Crystallogr.*, 2004, **60**, 134–141.
15 A. D. Rae, J. G. Thompson and R. L. Withers, *Acta Crystallogr., Sect. B: Struct. Sci.*, 1992, **48**, 418–428.
16 S. N. Ruddlesden and P. Popper, *Acta Crystallogr.*, 1958, **11**, 54–55.
17 J. S. Barnard, A. S. Eggeman, T. A. White, J. Sharp and P. A. Midgley, *Philos. Mag.*, 2010, **90**, 4711–4730.
18 M. Elcombe, E. H. Kisi, K. D. Hawkins, T. J. White, P. Goodman and S. Matheson, *Acta Crystallogr., Sect. B: Struct. Sci.*, 1991, **47**, 305–314.
19 H. Hughes, M. M. B. Allix, C. A. Bridges, J. B. Claridge, X. Kuang, H. Niu, S. Taylor, W. Song and M. J. Rosseinsky, *J. Am. Chem. Soc.*, 2005, **127**, 13790–13791.
20 R. Seshadri, C. Martin, A. Maignan, M. Hervieu, B. Raven and C. N. R. Rao, *J. Mater. Chem.*, 1996, **6**, 1585–1590.
21 P. D. Battle, M. A. Green, N. S. Laskey, N. Kasmir, J. E. Millburn, L. E. Spring, S. P. Sullivan, M. J. Rosseinsky and J. F. Vente, *J. Mater. Chem.*, 1997, **7**, 977–988.
22 T. Yokosawa, A. A. Belik, T. Asaka, K. Kimoto, E. Takayama-Muromachi and Y. Matsui, *Phys. Rev. B: Condens. Matter Mater. Phys.*, 2008, **77**, 024111.
23 N. A. Benedek and C. J. Fennie.
24 R. Vincent, D. M. Bird and J. W. Steeds, *Phil. Mag. A*, 1984, **50**, 745–752.